LOW FREQUENCY SAMPLING ADAPTIVE THRESHOLDING FOR FREE-SPACE OPTICAL COMMUNICATION RECEIVERS WITH MULTIPLICATIVE NOISE

H. R. Burris[1], C. Moore[2], M. Vilcheck[2], R. Mahon[3], M. Stell[1], M. Suite[2], M. Davis[4], W. Scharpf[2], A. Reed[2], W. Rabinovich[5], C. Gilbreath[6], E. Oh[6], N. M. Namazi[7]

1) Research Support Instruments, Inc., 4325-B Forbes Blvd., Lanham, MD. 20706
2) U.S. Naval Research Laboratory, Code 8123, Advanced Technology Branch, 4555 Overlook Ave., SW, Washington, D.C. 20375
3) Jaycor/Titan, Inc., 1410 Spring Hill Rd., McLean, VA. 22102.
4) Honeywell T.S.I., 7515 Mission Drive, Lanham, MD 20706
5) U.S. Naval Research Laboratory, Code 5654, Photonics Technology Branch, 4555 Overlook Ave., SW, Washington, D.C. 20375
6) U.S. Naval Research Laboratory, Code 7215, Radio/IR/Optical Sensors Branch, 4555 Overlook Ave., SW, Washington, D.C. 20375
7) The Catholic University of America, EECS Dept., Washington, D.C., 20064.

ABSTRACT

An adaptive thresholding method is presented for optimum detection for optical receivers with large multiplicative noise. The technique uses low frequency sampling of the detected current that enables calculation of the bit means and variances and estimation of the optimum detection threshold. The regime in which this holds is when the sampling frequency is lower than the bit rate but higher than atmospheric turbulence frequency content. Simulations are done with data obtained from the NRL Chesapeake Bay Lasercomm Testbed. The results of simulations comparing BER performance versus sample rate and parameter estimation error will be presented. If the system parameters are characterized in advance with reasonable accuracy, the BER obtained will typically be an order of magnitude improvement over the equal variance threshold (depending on the signal to noise ratio).

Keywords: optical communications; adaptive threshold; adaptive signal processing.

1. INTRODUCTION

It is well known that the optimum detection threshold for optical receivers with large multiplicative noise components (i.e. signal dependant noise) is not simply the average value of the high and low bit currents (or zero for ac coupled detectors). The optimum detection threshold in this type of system is derived from a Bayes' likelihood ratio test (LRT) and is a function of the bit level means and variances; therefore, it will not be constant under varying transmission conditions [1,2]. Optical detectors exhibiting this characteristic are avalanche photodiodes (APD's) and photomultipliers as well as PIN photodiodes coupled with optical preamplifiers [2,3,4,5]. The derivation of the detection threshold requires a priori knowledge of the mean and variance of the bit levels. As stated above, in free-space optical communication links this will be problematic. An adaptive method that can track the changes in the mean and variance of the signal bits, and update the detection threshold is needed in order to implement the multiplicative noise Bayesian LRT detection threshold [3,6].

In free-space optical communication (FSO) systems, it is usually desirable to have the sensitivity of the detector as high as possible to reduce the required laser power for a
specified link margin. However, the optical receivers used for high speed optical communication systems that operate closest to the quantum limit are the PIN diode coupled to an optical fiber preamplifier and an APD. Both of these devices have large multiplicative noise components that cannot be ignored.

Free-Space Laser Communication and Active Laser Illumination III,
edited by David G. Voelz, Jennifer C. Ricklin, Proc. of SPIE Vol. 5160
(SPIE, Bellingham, WA, 2004) · 0277-786X/04/$15 · doi: 10.1117/12.507553

Report Documentation Page			*Form Approved OMB No. 0704-0188*

1. REPORT DATE **2004**	2. REPORT TYPE	3. DATES COVERED **00-00-2004 to 00-00-2004**
4. TITLE AND SUBTITLE **Low Frequency Sampling Adaptive Thresholding for Free-Space Optical Communication Receivers with Multiplicative Noise**		5a. CONTRACT NUMBER 5b. GRANT NUMBER 5c. PROGRAM ELEMENT NUMBER
6. AUTHOR(S)		5d. PROJECT NUMBER 5e. TASK NUMBER 5f. WORK UNIT NUMBER
7. PERFORMING ORGANIZATION NAME(S) AND ADDRESS(ES) **Naval Research Laboratory,Code 8123,4555 Overlook Avenue, SW,Washington,DC,20375**		8. PERFORMING ORGANIZATION REPORT NUMBER
9. SPONSORING/MONITORING AGENCY NAME(S) AND ADDRESS(ES)		10. SPONSOR/MONITOR’S ACRONYM(S) 11. SPONSOR/MONITOR’S REPORT NUMBER(S)

12. DISTRIBUTION/AVAILABILITY STATEMENT
Approved for public release; distribution unlimited

13. SUPPLEMENTARY NOTES
The original document contains color images.

14. ABSTRACT

15. SUBJECT TERMS

16. SECURITY CLASSIFICATION OF:			17. LIMITATION OF ABSTRACT	18. NUMBER OF PAGES	19a. NAME OF RESPONSIBLE PERSON
a. REPORT **unclassified**	b. ABSTRACT **unclassified**	c. THIS PAGE **unclassified**		**14**	

In previous work, several adaptive predictor methods have been developed which estimate both the mean and the variance of the bit levels well enough to produce bit error rate performance at the theoretical limit [7,8]. These methods include Kalman filtering for single or multiple samples per bit, least mean squares (LMS) adaptive algorithm, and a modified sequential regression (SER) adaptive algorithm. These adaptive signal processing algorithms require high speed sampling equipment and high speed computers for implementation. Since this type of equipment can be costly and difficult to implement, it is desired to find a method of implementing adaptive thresholding that is simple and reasonably cost effective. The purpose of the work discussed in this paper is to develop an inexpensive implementation method for a lower bit rate optical link such as an asymmetric 100 Mbps link based on a multiple quantum well (MQW) modulating retroreflector device [9]. Since these lightweight devices are possible candidates for portable links, an APD would increase the sensitivity of the interrogator without adding weight, while reducing the required transmitter laser power.

2. BACKGROUND

As stated above, the optimum detection threshold for an optical detector with signal dependant noise that cannot be ignored can be derived from a Bayes' Likelihood Ratio Test [7,8]. The expression for the optimum threshold is

$$\gamma = \frac{\sigma_0 \cdot \sigma_1}{\sigma_1^2 - \sigma_0^2} \cdot \sqrt{\left(\mu_1 - \mu_0\right)^2 + 2 \cdot \left(\sigma_1^2 - \sigma_0^2\right) \cdot \ln\left(\sigma_1 / \sigma_0\right)} + \frac{\mu_0 \cdot \sigma_1^2 - \mu_1 \cdot \sigma_0^2}{\sigma_1^2 - \sigma_0^2} \qquad (1)$$

in which μ_0 and μ_1 are the mean signal currents of the low and high bits respectively and the σ_0^2 and σ_1^2 are the respective variances. If the signal dependant noise is negligible as it is in a standard PIN diode (with no optical amplifier), σ_0^2 and σ_1^2 are approximately equal and the Eqn. (1) will reduce to the average value of μ_0 and $\mu_{1.}$ This approximation is the equal variance threshold (EVT).

The APD has an increased shot noise due to the avalanche gain process. The APD shot noise current variance is modeled as:

$$\sigma_{sh,apd}{}^2 = 2 \cdot e \cdot G_m{}^2 \cdot F\left(G_m\right) \cdot R \cdot P_r \cdot B_e \qquad (2)$$

where G_m is the avalanche multiplicative gain, P_r is the received optical power, B_e is the electronic bandwidth, R is the detector responsivity at a gain of 1, and $F(G_m)$ is the excess noise factor which is a function of the avalanche gain. The APD shot noise is typically modeled as a zero mean, Gaussian process at the signal levels encountered in optical communication systems. The excess noise factor is given by:

$$F\left(G_m\right) = k_A \cdot G_m + \left(1 - k_A\right) \cdot \left(2 - 1/G_m\right) \qquad (3)$$

where k_A is the ionization coefficient which is a property of the semiconductor material used in the APD and has a range from 0 to 1. In silicon APD's, which can be used up to an optical wavelength of ~ 1100nm, the ionization coefficient can be kept fairly small (typically << 1). However, for optical wavelengths above ~ 1100 nm, such as 1330 nm and 1550 nm which are of particular interest for freespace links, other semiconductor materials, such as InGaAs, are used. InGaAs, APD's have an ionization coefficient much higher than that of silicon, typically in the vicinity of ~ 0.7 [10,11]. Therefore, since the signal dependent shot noise in APD's is multiplied by an additional factor of $G_m{}^2 \cdot F\left(G_m\right)$, the shot noise in these devices will dominate over thermal noise and cannot be neglected.

In the PIN diode-optical preamp receiver, there will be additional terms in the current noise variance due to the beating of the spontaneous noise power produced in the optical amplifier with itself and with the received optical signal. These noise terms can also be adequately modeled as Gaussian processes and, at typical optical amplifier gains, will be the dominant noise terms over both thermal noise and shot noise. The signal-spontaneous beat noise produces a noise current variance of:

$$\sigma_{sig-spont}{}^2 = 4 \cdot R^2 \cdot G_o \cdot P_r \cdot P_n \cdot \left(G_o - 1\right) \cdot B_e \qquad (4)$$

where G_o is the optical amplifier gain and $P_n = n_{sp} \cdot h \cdot \nu_c$, in which h is Planck's constant, ν_c is the optical frequency, and n_{sp} is the spontaneous emission factor (typically in the range of 2 to 5) [10]. The spontaneous-spontaneous beat noise produces a noise current variance of:

$$\sigma_{spont-spont}{}^2 = 2 \cdot R^2 \cdot \left[P_n \cdot (G_o - 1) \right]^2 \cdot (2 \cdot B_o - B_e) \cdot B_e \qquad (5)$$

in which B_o is the optical bandwidth of the system, usually determined by optical bandpass filters. In practice, to reduce the system noise and improve performance, the spontaneous-spontaneous beat noise term can usually be reduced to a very small level with optical filters so that the dominant noise term is always the signal-spontaneous beat noise. As can be seen above, this dominant noise term is also proportional to the received optical power.

As shown above, the most sensitive detector configurations for freespace optical communication systems have large multiplicative (signal dependent) noise variances which cannot be ignored. Although the PIN-diode-optical-preamp receiver has a sensitivity closest to the quantum limit, the APD receiver has a much wider use in FSO. Currently, optical preamplifiers are constructed with single-mode optical fiber. In freespace optical systems, turbulence-induced spot motion makes coupling of received light into a single-mode fiber extremely difficult and the sensitivity gain is canceled by the coupling. Therefore, the analysis and simulations done for this paper concentrates on systems using APD detectors.

Atmospheric turbulence can cause the average received power to fluctuate with power spectrum components in the kilohertz regime. Therefore, the received bit signal currents and their variances fluctuate as well. In order to maintain the receiver detection threshold at near-optimum, these bit-level means and variances must be tracked and estimated. A block diagram of a proposed solution is shown below in Figure 1.

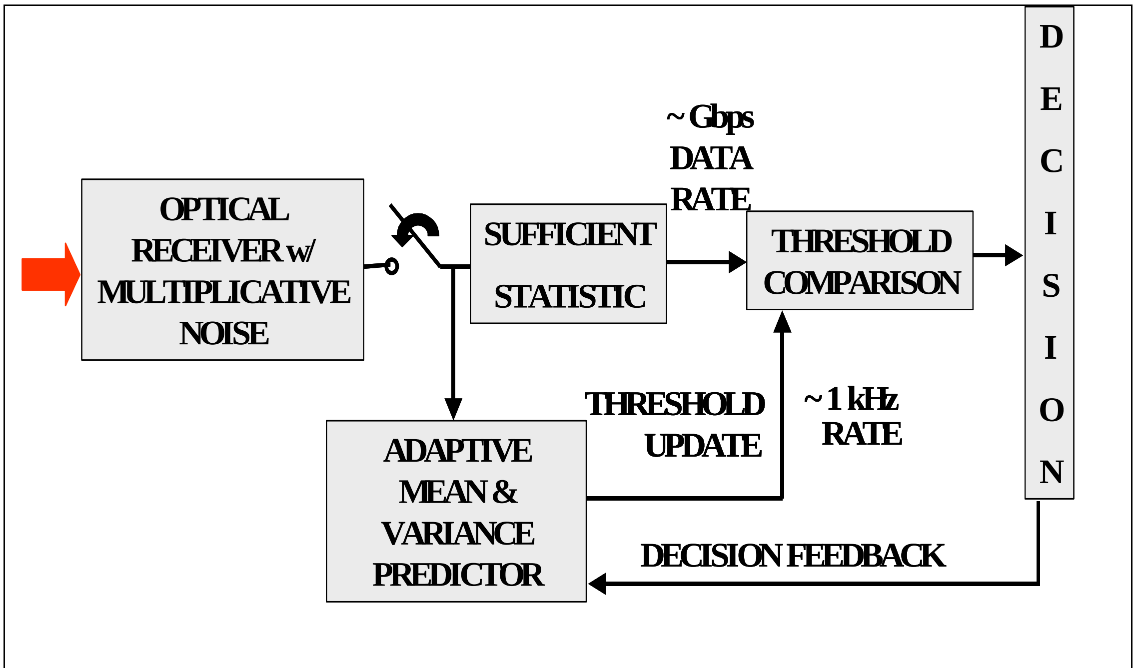

Figure 1: Adaptive System Block Diagram

Previous work has involved theoretical comparisons of bit error rates obtainable with the optimum Bayesian LRT detection threshold and the equal variance threshold. An example of this sort of analysis is shown in Figure 2 in which it can be seen that more than an order of magnitude improvement can be obtained with the adaptive LRT threshold [7,8]. It has also been shown that use of an LRT threshold, established at some fixed value, and not updated over time, will actually perform worse than an EVT threshold [7,8].

These past efforts [7,8] have concentrated on development of adaptive predictor algorithms which can predict the mean and variance values and maintain the detection threshold near optimum. Adaptive algorithms have been developed based on Kalman Filters, Least Mean Squares adaptive predictors, and a Modified Sequential Regression adaptive algorithm. It has been demonstrated with simulation studies that these adaptive predictors can yield BER performance at the theoretical limit, with order-of-magnitude improvement over the EVT threshold performance. Figure 3 shows a comparison of the three adaptive predictors' BER performance to the theoretical limit. Figure 4 is a comparison of the Kalman Filter adaptive predictor BER performance to that of the EVT threshold. The results were generated with simulated bit data superimposed on actual power fade rate data taken at the NRL Free-space Lasercomm Test Facility at Chesapeake Beach, MD [7,8].

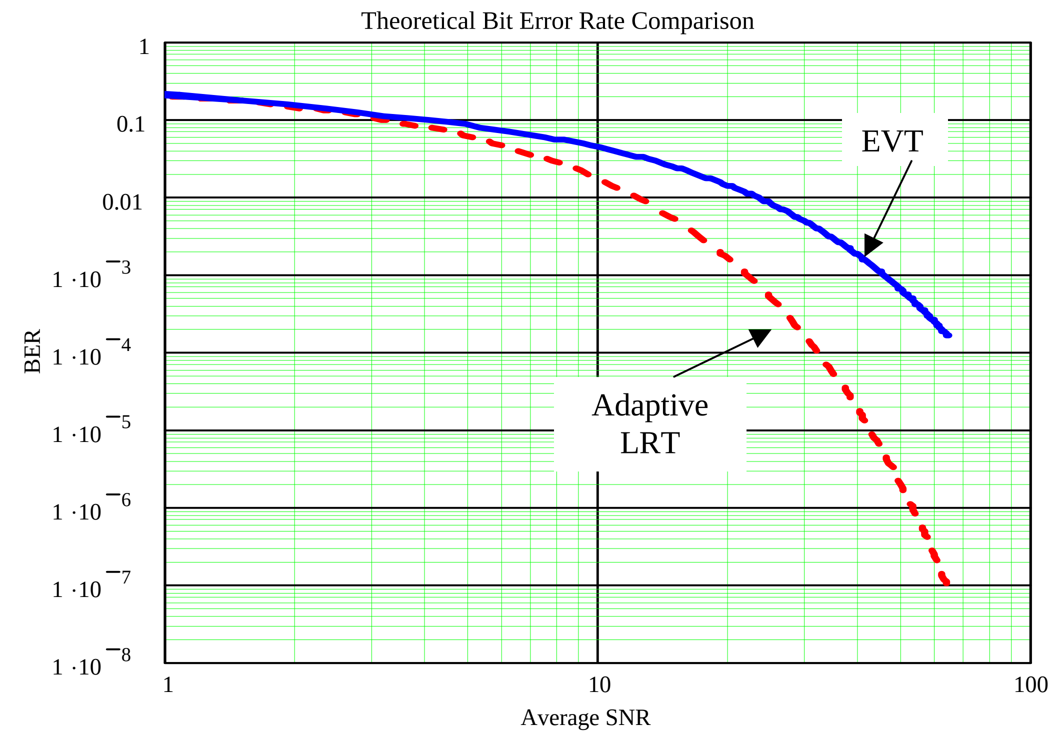

Figure 2: Comparison of theoretical bit error rate curves for the adaptive LRT and the EVT. The upper solid curve is the BER curve for a EVT type threshold (equal variances). The lower dashed curve uses a Bayes' LRT threshold.

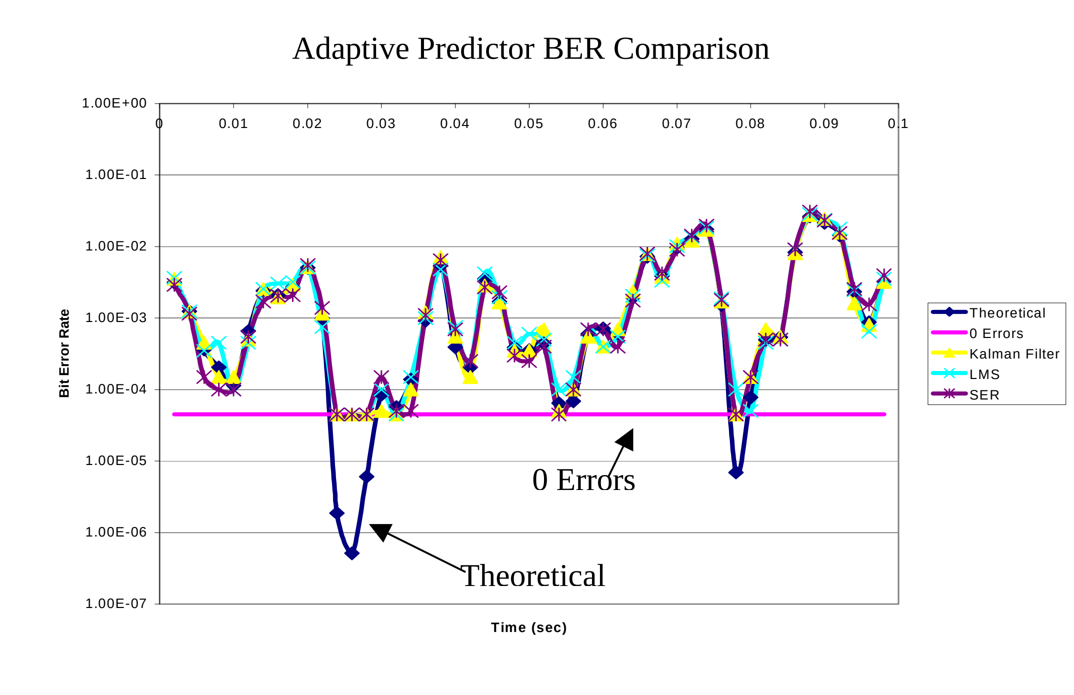

Figure 3: Comparison of Theory, Linear State Model Kalman filter, LMS predictor and Modified Sequential Regression predictor bit error rate performance; averaged over 2msec time intervals.

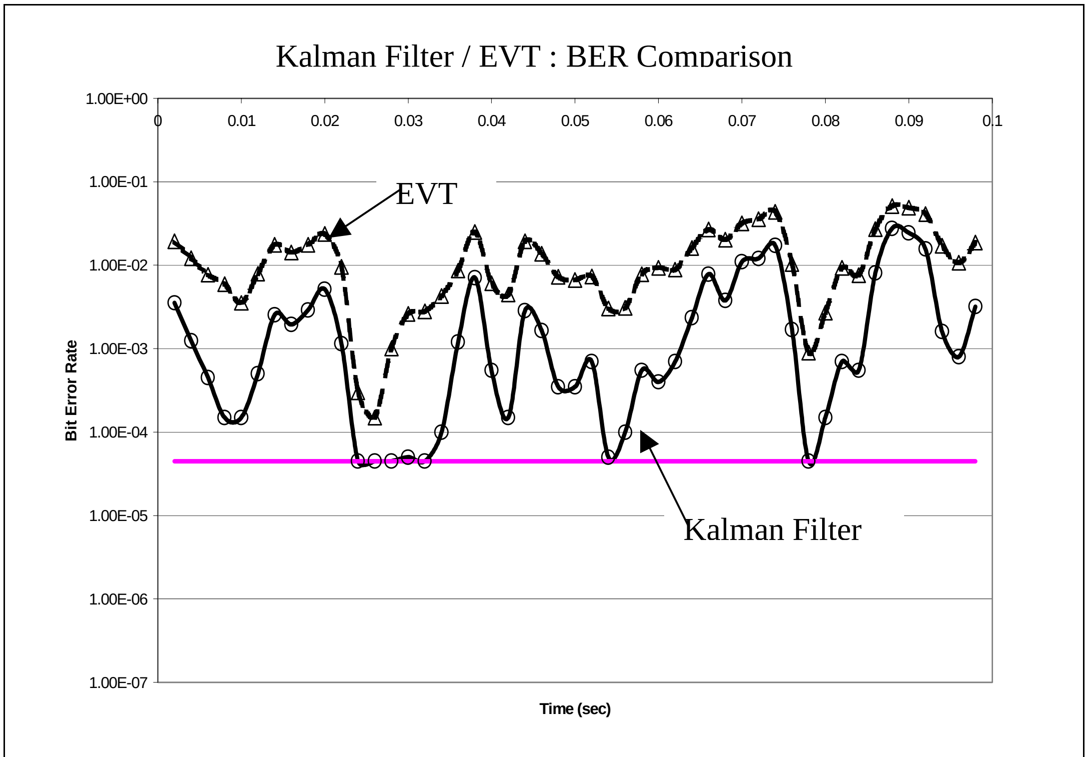

Figure 4: Comparison of Kalman filter BER performance with the EVT.

3. LOW FREQUENCY SAMPLING

Implementation of the adaptive predictors described above requires high speed sampling and high speed computing ability. These processing requirements can be very costly and difficult to realize.
It is desired to find a way to implement adaptive thresholding that is cheaper and easier. If the free-space optical link components can be well characterized in advance, it is possible to estimate the optimum detection threshold by estimating the average received detector current before AC coupling. For a communication link using an APD, the parameters which must be known or estimated in advance are: transmitted contrast ratio, non-multiplicative circuit noise variance, APD gain, APD ionization ratio, APD excess noise factor, and APD bandwidth. These parameters are accessible from manufacturer's specifications or measurement. With these parameters known or estimated, and with a continuous measurement of the receiver detector current, the high and low bit mean and variance levels can be calculated. Consequently, calculation (estimation) of the optimum detection threshold is enabled.

A testbed is being developed at the Naval Research Laboratory to test the feasibility of this method in the laboratory. The average receiver current will be estimated by low frequency sampling of the received signal before AC coupling with a commercial, off-the-shelf (COTS) Analog-to-Digital (A/D) card from National Instruments. A block diagram is shown in Figure 5. System parameters will be characterized in advance and the estimated optimum detection threshold will be updated with a COTS D/A card and a COTS Data and Clock Recovery chip. Data and Clock Recovery chips may be obtained that have a control voltage input for adjusting the detection threshold used in the data recovery.

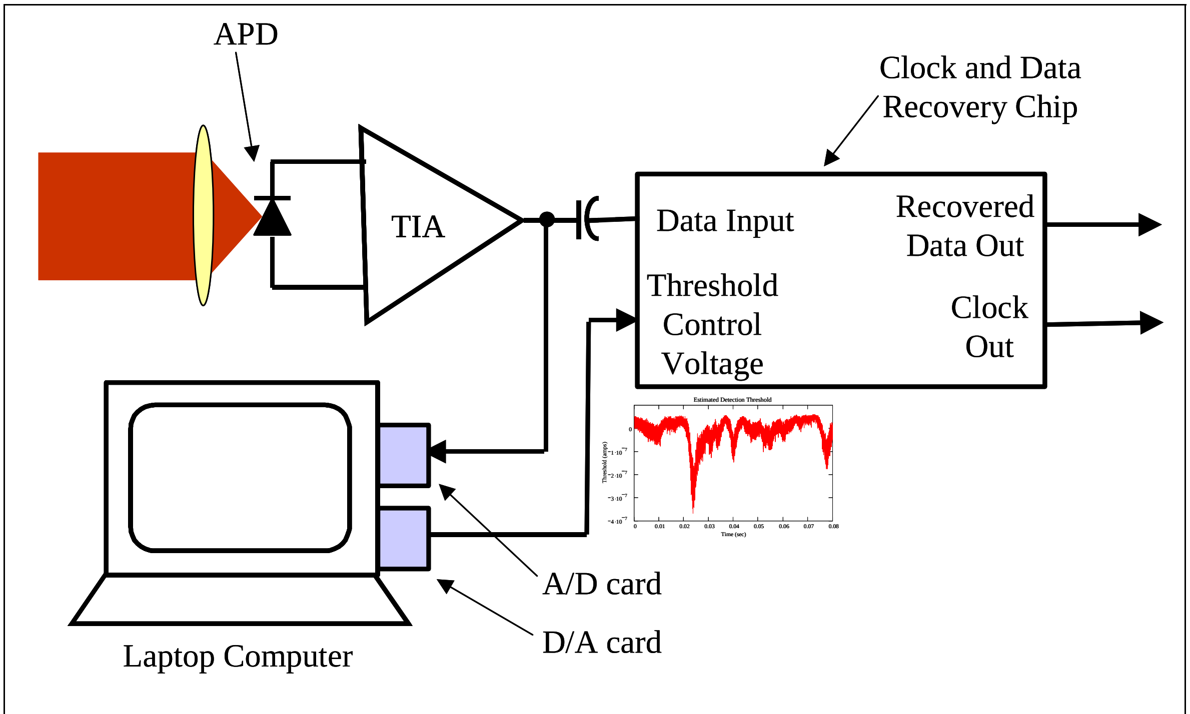

Figure 5: Block diagram of low frequency sampling testbed being developed at NRL.

4. SIMULATION RESULTS

As previously stated, studies were performed with data consisting of a random bit pattern imposed on power fade rate data taken at the NRL Lasercomm Test Facility. The average receiver current was estimated at sampling rates of 1, 2, 5, 10, 50, 100, and 500 kHz using the simulated input data. The estimated receiver current was then used to calculate the estimate of the optimum detection threshold. The estimated thresholds were used to detect the bits on the AC coupled

data. The detected bits were compared to the true transmitted bit sequence and the BER was compared to that obtained with the true optimum detection threshold. These studies of BER as a function of sampling frequency were performed for two average signal-to-noise ratios (SNR) of 17 and 43. The different SNR values were obtained by scaling the original digitized fade rate data before generating the simulation data. The simulation data (4 million bits) was generated by the process depicted in Figure 6. The parameters used in the data generation process correspond to COTS components; specifically: an OCP STX-12 transmitter module operating at 1550nm with a contrast ratio of 10dB and a Lucent Technologies 126C InGaAs APD.

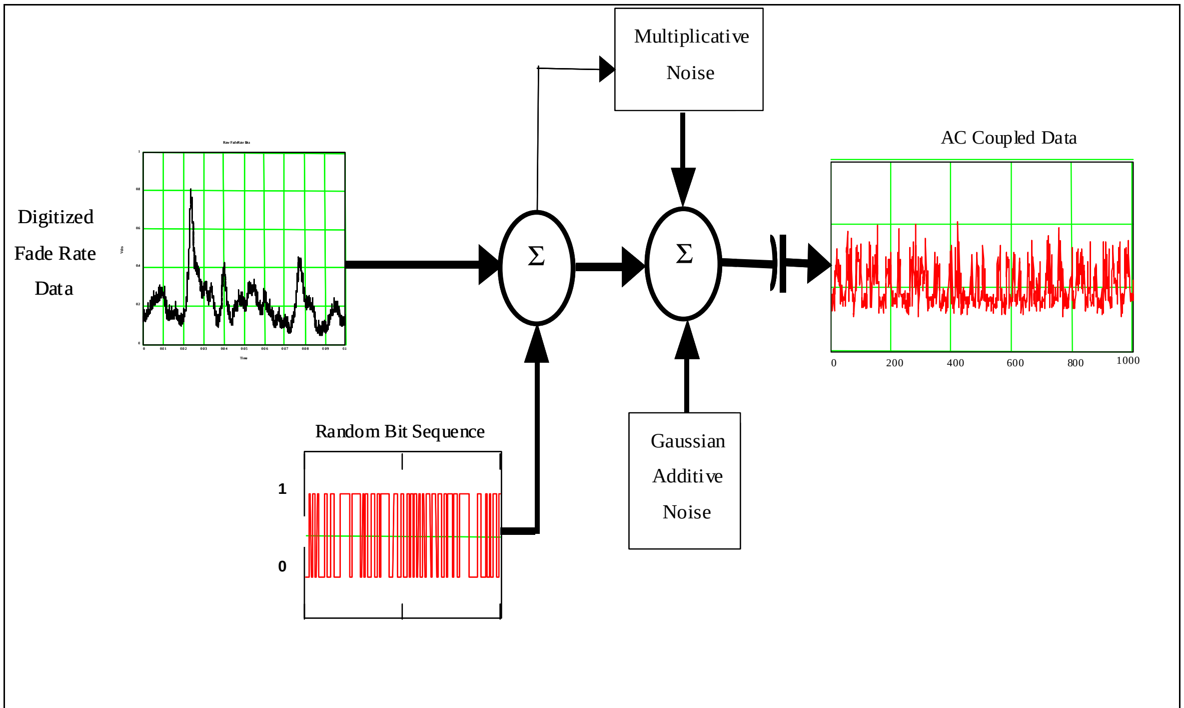

Figure 6: Simulation data generation process.

Figure 7 contains a graph of the true optimum detection threshold for the case of average SNR of 17. In the graph, it is shown that the detector threshold value is in the microamps regime. Although the simulations were done using detector current, in reality, the detector current will be multiplied by the trans-impedance gain of the trans-impedance amplifier (TIA). This factor has no effect on the simulation outcome (other than a slight decrease in SNR) since the TIA gain is simply a multiplier of the current and threshold for implementation. Figure 7 is the true optimum detection threshold for the data set being used for the average SNR = 17 case and should be compared with the estimates obtained by low frequency sampling in figures 9 and 10.

Figure 8 is an example of the AC coupled data that is used in the simulation experiment at an average SNR of 17. The plot in Figure 8 plots every tenth data sample in the 4 million generated. The power fluctuations caused by turbulence are apparent as are the effects of the multiplicative noise; i.e. the “one” bits are more noisy than the “zero” bits and the plot is not symmetric about the x-axis.

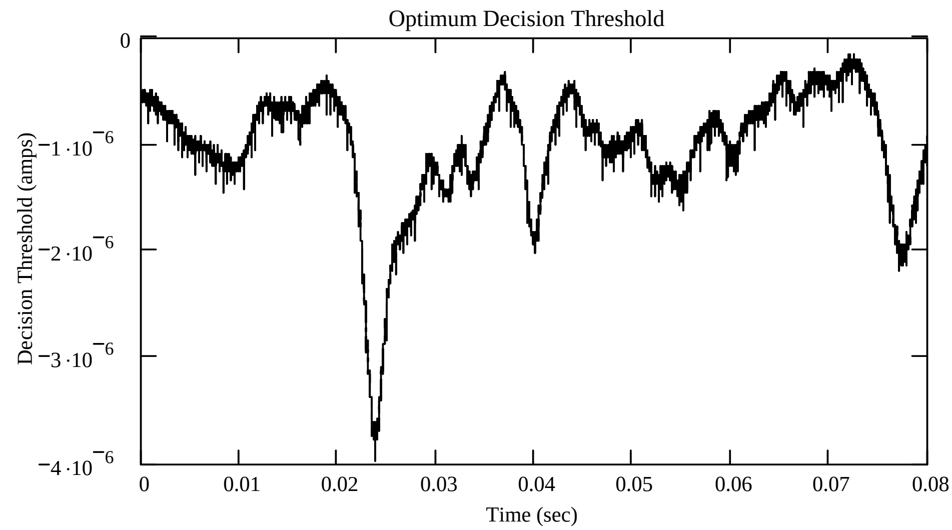

Figure 7: True optimum decision threshold; SNR ave =17.

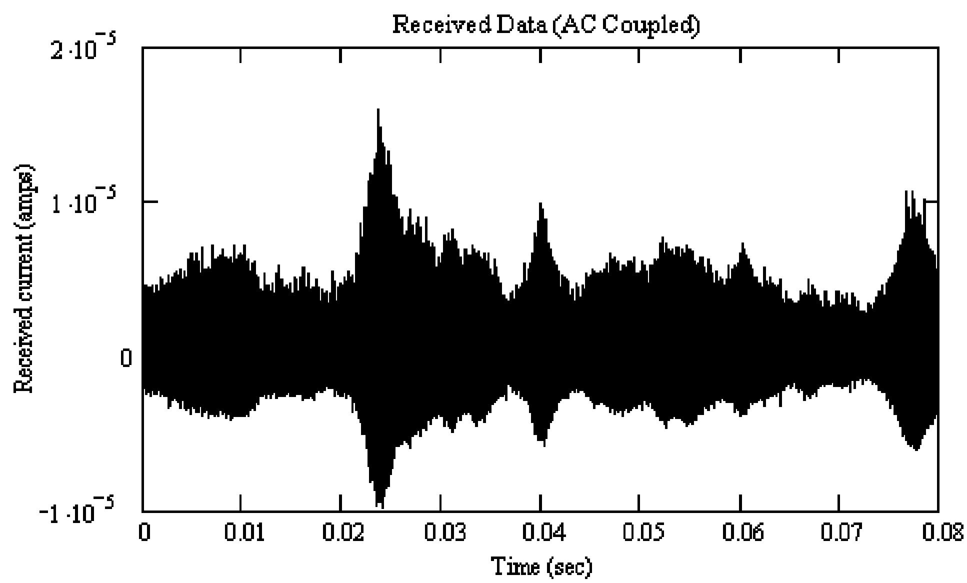

Figure 8: AC coupled received data; SNR ave = 17.

Figures 9 and 10 are examples of the estimated receiver current and estimated optimum detection threshold for SNR=17, for two different sample rates, 5 and 500 kHz. Estimated detection thresholds were obtained for a range of sampling frequencies from 1 kHz to 500 kHz. These were determined from the estimates of the receiver current and the predetermined or estimated values of the transmitter and receiver parameters such as contrast ratio and APD gain.

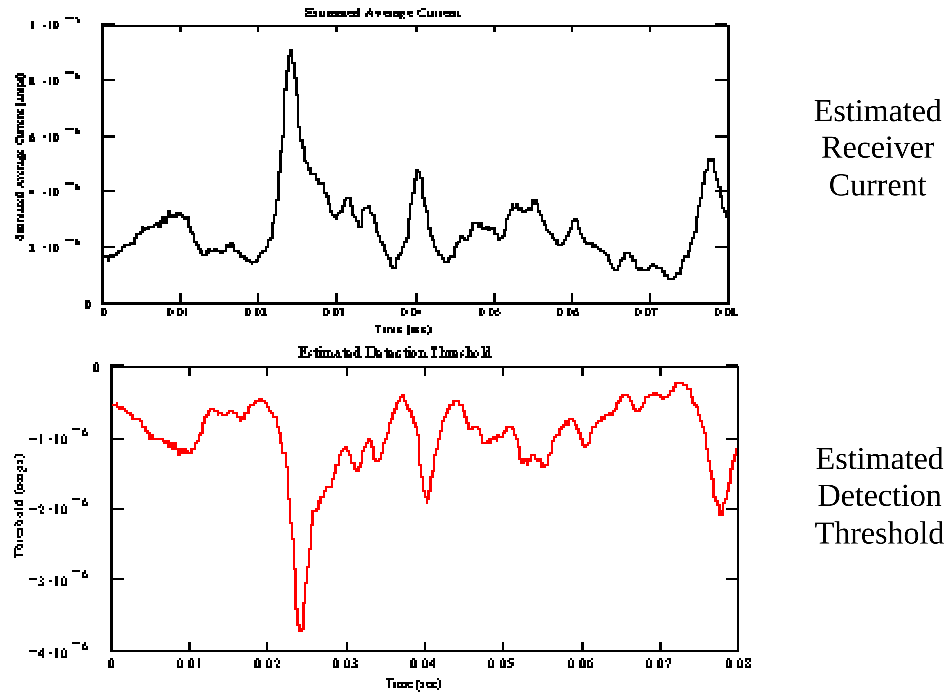

Figure 9: Estimated receiver current and estimated detection threshold; Sample frequency = 5 kHz; SNR ave = 17.

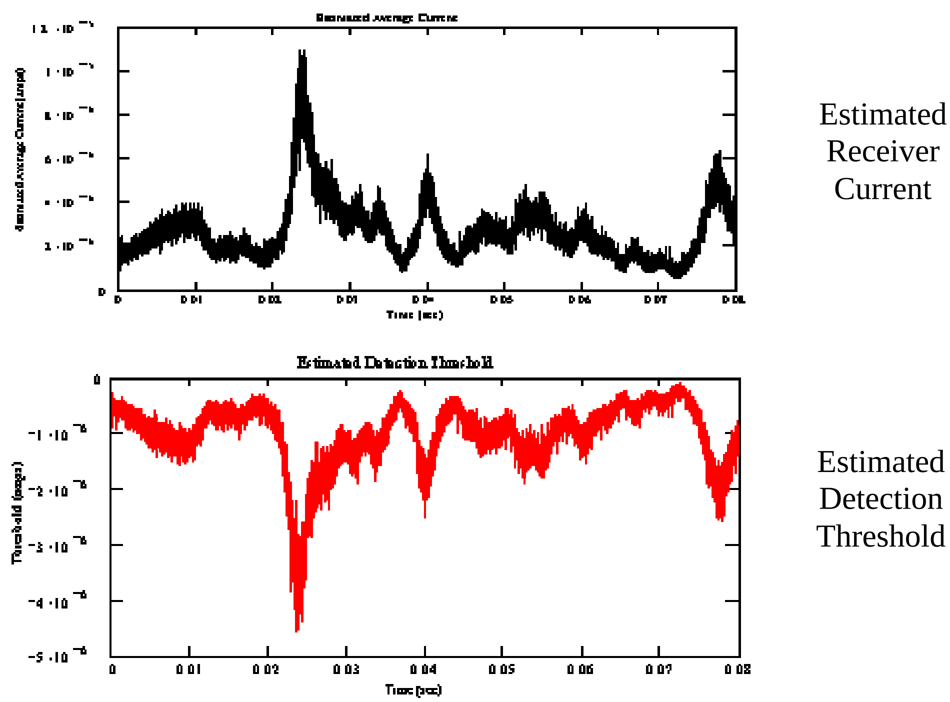

Figure 10: Estimated receiver current and estimated detection threshold; Sample frequency = 500 kHz; SNR ave = 17.

To obtain the data shown in Figures 11 and 12, the estimated detection thresholds for the various sampling frequencies were used to detect the bits in the AC coupled data. These detected bits were then compared to the true transmitted bit stream to determine average bit error rate. The data was scaled to obtain SNR values that would result in average bit error rates greater than 1×10^{-4}. This is the region in figure 2 in which the theoretical curves for the optimum threshold and for the EVT threshold are fairly close together so that small changes in BER performance are obvious. The lower straight line in these figures is the BER obtained by using the true optimum detection threshold. The BER obtained by using the EVT threshold is listed in the upper right corner of the graphs. As can be seen in the figures, if the sampling frequency of the received current monitor is 10 kHz or higher, the BER performance will be very close to that obtained with the true optimum detection threshold and depending on the SNR, an order of magnitude improvement would be obtained compared to the EVT threshold.

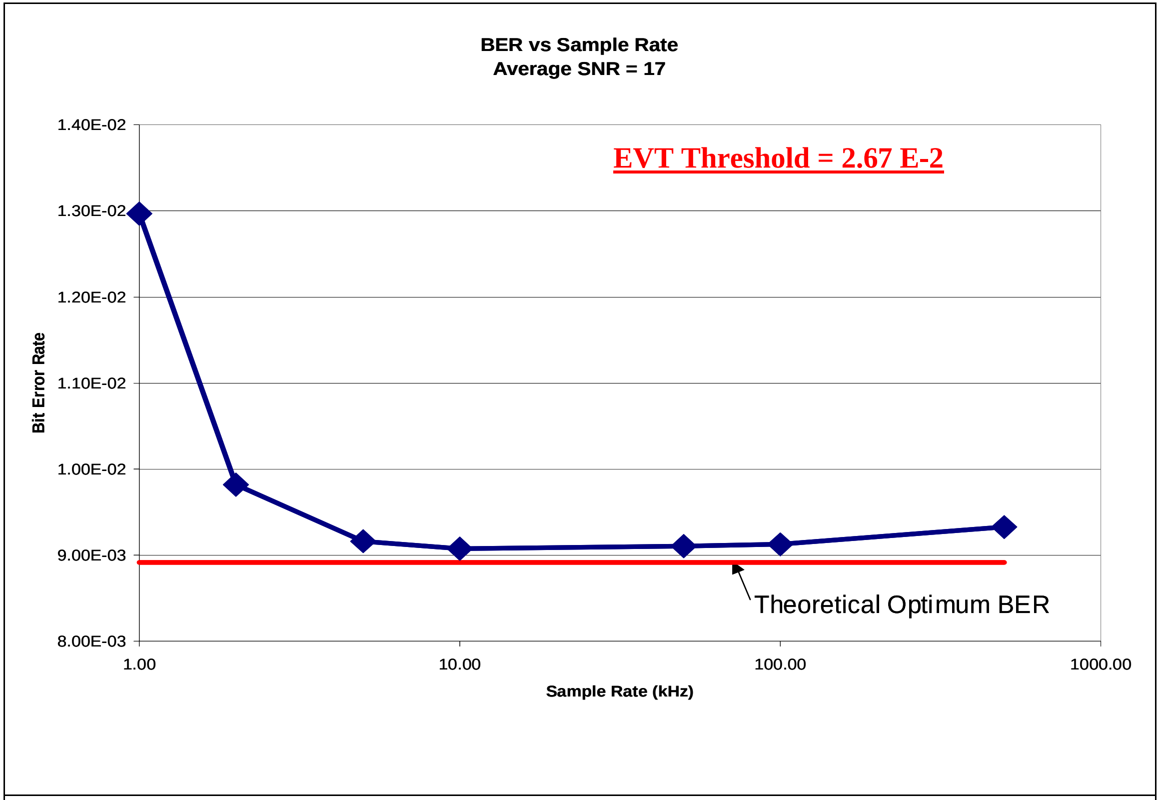

Figure 11: BER versus sample rate of receiver current; SNR ave = 17.

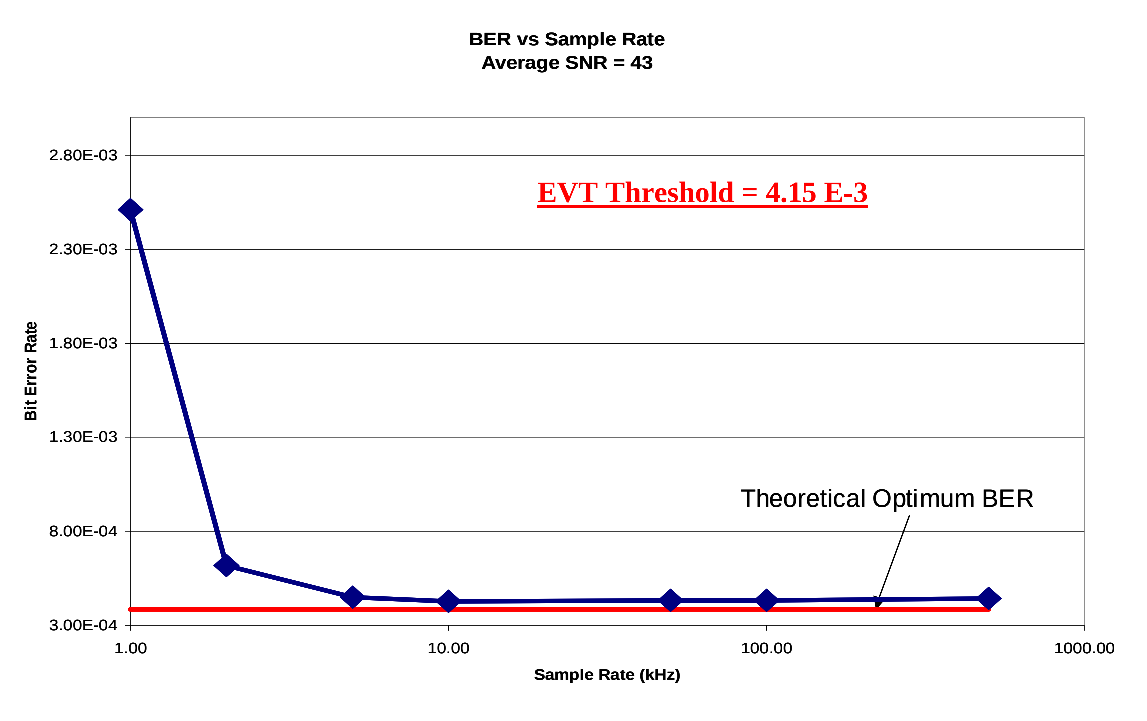

Figure 12: BER versus sample rate of receiver current; SNR ave = 43.

Since certain system parameters discussed above are required to be known a priori in order to calculate the detection threshold, it is desirable to have an understanding of the accuracy with which these parameters need to be known. Since APD gain and the contrast ratio of the transmitter have a large effect both on the mean and the variance of the bit levels, simulation studies were performed in which these parameters were intentionally changed from the true value to determine the effect on the detection threshold and BER. The studies were done for two different average SNR values (12 and 59) and for parameter estimation errors of +/–50%. The sampling frequency used for these simulations was 50 kHz and the total number of bits used was 500,000.

Figure 13 shows the results for these parameters. The side-by-side graphs contain the same data but with different scales so that a comparison to the EVT-threshold BER could be done in the graph on the right. The higher average SNR case (SNR = 59) has a two level graph that is the difference between one error and two errors out of 500,000 bits. This indicates that in the high SNR case, the BER is not very sensitive to errors in the detection threshold due to gain estimation errors. Figure 14 is the simulation results for errors in the estimate of the contrast ratio. As in Figure 13, the upper two graphs are for the lower average SNR of 12 and the lower two graphs are for the average SNR of 59. It is shown that an overestimate of the contrast ratio can result in a large increase in the BER, as one would expect.

It should be noted that in the analysis, the received current estimates were obtained by averaging over the integration time of the A/D card. It was assumed that the integration time was equal to the inverse of the sample frequency. An attempt was made to use an LMS linear transversal filter as a predictor with the averaged current values as inputs to improve the estimation of the detection threshold. However, this resulted in little or no improvement in the BER, so the measured average current value was used as the prediction of received current.

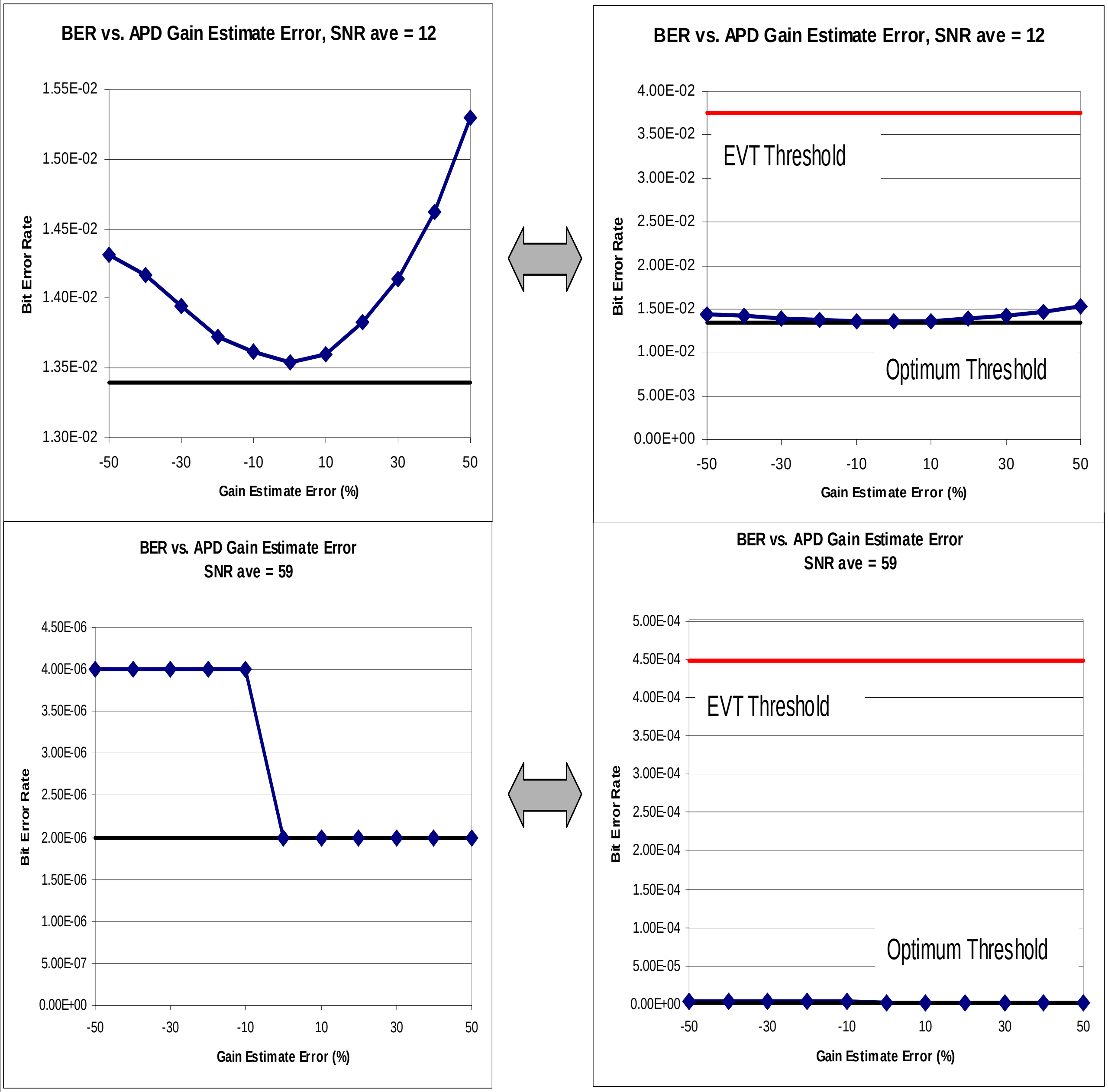

Figure 13: Effects of APD gain estimate error.

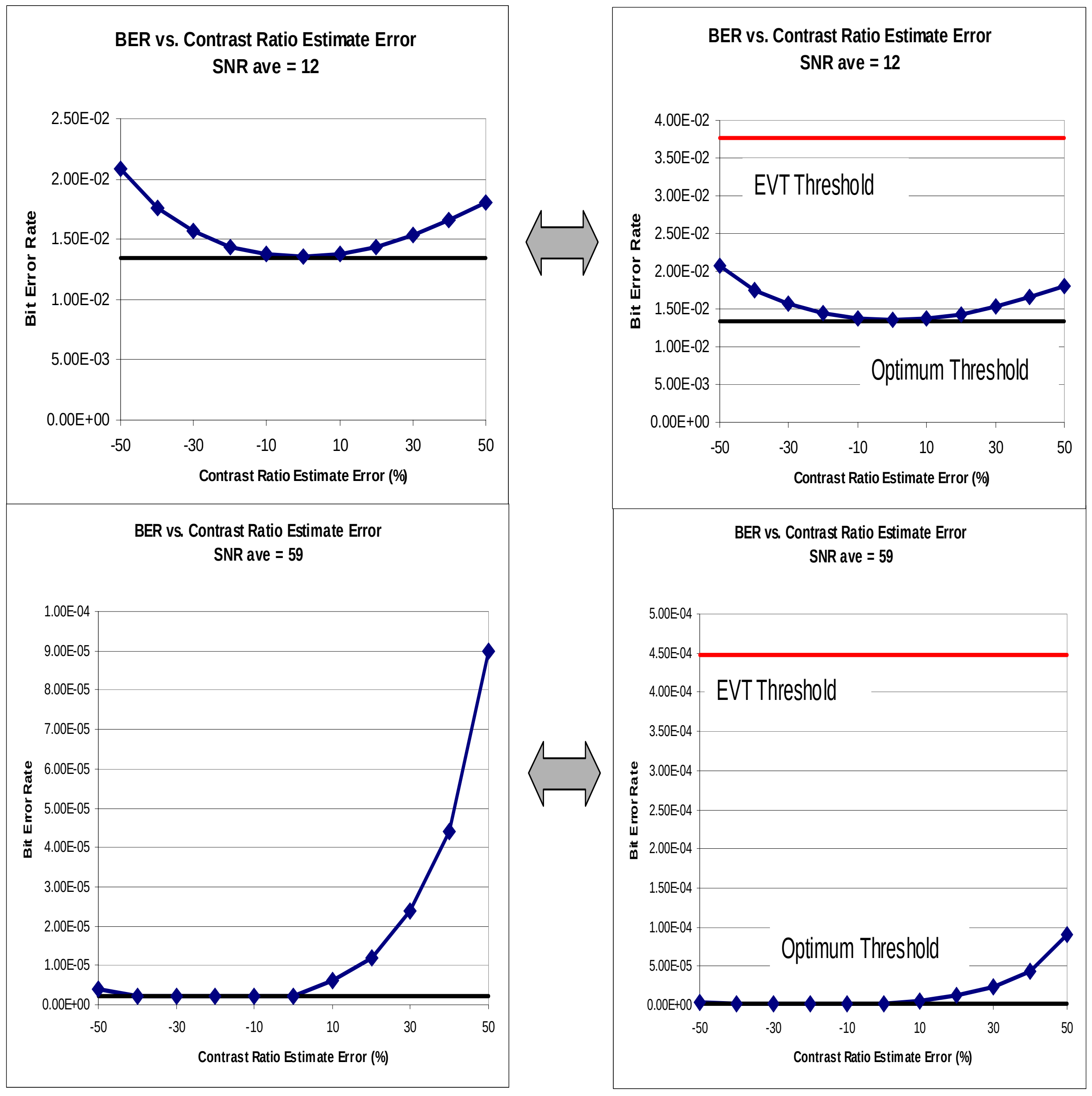

Figure 14: Effects of contrast ratio estimate error.

5. CONCLUSIONS

With low frequency sampling of the received detector current, an estimation of the detection threshold can be obtained which is usefully comparable to that obtained with the true optimum detection threshold. If the system parameters are characterized in advance with reasonable accuracy (+ /- 10%), the BER obtained will typically be an order of magnitude improvement over the EVT threshold (depending on the SNR). These results were verified with a simulated data sequence and real fade-rate data obtained over a 16.2 km link (32.4 km round trip off of retroreflectors) at the NRL FSO facility. These preliminary findings indicate that adaptive thresholding may be implemented to improve BER in a free

space optical link with significantly less intensive computational loads and commensurately lower costs. In future work, we will conduct experiments to verify these results.

6. BIBLIOGRAPHY

1. Andrews, Larry C., and Phillips, Ronald L., *Laser Beam Propagation Through Random Media*, SPIE Optical Engineering Press, 1998.
2. Harres, D., “Nonlinear Processing of Manchester Data Corrupted by Multiplicative Noise”, *IEEE International Conference on Communications*, pp. 683-687, July 1998.
3. Harres, D., “Algorithm decreases BER of optically encoded Manchester data”, *EDN*, pp. 47-55, December 1999.
4. McIntyre, R. J., “Multiplication Noise in Uniform Avalanche Diodes”, *IEEE Transactions on Electron Devices*, vol. ED-13, pp. 164-168, January 1966.
5. Olsson, N. A., “Lightwave Systems With Optical Amplifiers”, *Journal of Lightwave Technology*, Vol. 7, No. 7, pp. 1071-1082, July 1989.
6. Brown, William C., “Optimum Thresholds for Optical On-Off Keying Receivers Operating in the Turbulent Atmosphere”, Proceedings of SPIE, Vol. 2990, February 1997.
7. Burris, H.R., et. al., "A Comparison of Adaptive Methods for Optimal Thresholding for Free-Space Optical Communication Receivers with Multiplicative Noise", *Proceedings of SPIE, Free-Space Laser Communication and Laser Imaging II*, July 2002.
8. Burris, H.R., et. al., "Adaptive Thresholding for Free-space Optical Communication Receivers with Multiplicative Noise", *IEEE Aerospace Conference Proceedings*, March 2002.
9. Mahon, R., et al, “A free-space optical communications link at 1550 nm using multiple quantum well modulating retro-reflectors in a marine environment”, *Proceedings of SPIE, Free-Space Laser Communication and Laser Imaging III*, August 2003.
10. Ramaswami, R, and Sivarajan, K.N., "*Optical Networks: A Practical Perspective*", Academic Press, 1998.
11. Alexander, Stephen B., *Optical Communication Receiver Design*, SPIE Optical Engineering Press, 1997.